

# Benzonitrile Adducts of Terminal Diarylphosphido Complexes: Preparative Sources of “Ru=PR<sub>2</sub>”

Marc-André M. Hoyle,<sup>†</sup> Dimitrios A. Pantazis,<sup>‡</sup> Hannah M. Burton,<sup>†</sup> Robert McDonald,<sup>§</sup> and Lisa Rosenberg<sup>\*†</sup>

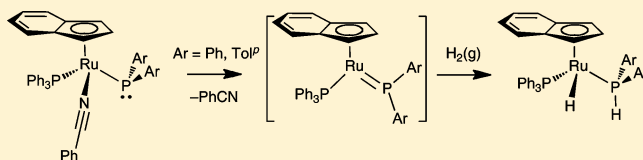
<sup>†</sup>Department of Chemistry, University of Victoria, P.O. Box 3065, Victoria, British Columbia, Canada V8W 3V6

<sup>‡</sup>Max Planck Institute for Bioinorganic Chemistry, Stiftstr. 34-36, 45470 Mülheim an der Ruhr, Germany

<sup>§</sup>X-ray Crystallography Laboratory, Department of Chemistry, University of Alberta, Edmonton, Alberta, Canada T6G 2G2

## Supporting Information

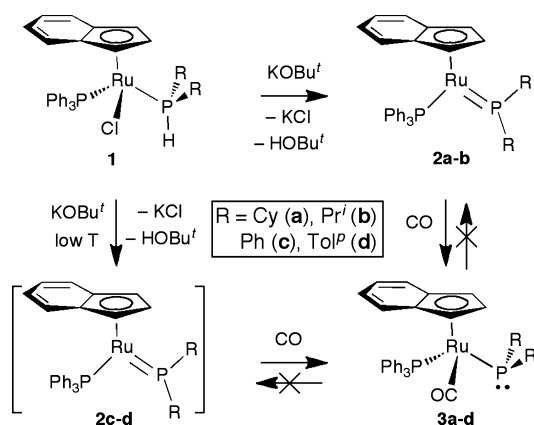
**ABSTRACT:** Dehydrohalogenation of secondary diarylphosphine ruthenium complexes in the presence of benzonitrile yields stable, isolable nitrile adducts of the formula [Ru( $\eta^5$ -indenyl)(PAR<sub>2</sub>)(NCPH)(PPh<sub>3</sub>)], in which the terminal phosphido ligand is pyramidal at P and contains a stereochemically active lone pair. Unlike the analogous carbonyl adducts [Ru( $\eta^5$ -indenyl)(PAR<sub>2</sub>)(CO)(PPh<sub>3</sub>)], these benzonitrile complexes behave as masked sources of the highly reactive planar phosphido complexes [Ru( $\eta^5$ -indenyl)(PAR<sub>2</sub>)(PPh<sub>3</sub>)], which contain a Ru=PAR<sub>2</sub>  $\pi$  bond. This is illustrated by the addition (or cycloaddition) reactions of the benzonitrile adducts with dihydrogen, methyl iodide, and 1-hexene, as well as their thermal decomposition via orthometalation of the PPh<sub>3</sub> ligand. Enthalpies of CO vs NCPH dissociation from the [Ru( $\eta^5$ -indenyl)(PR<sub>2</sub>)(PPh<sub>3</sub>)] fragments (R = alkyl, aryl) have been calculated, as has the trajectory of addition of H<sub>2</sub> to the model planar phosphido complex [Ru( $\eta^5$ -indenyl)(PMe<sub>2</sub>)(PMe<sub>3</sub>)]. The latter study shows the intermediacy of an  $\eta^2$ -H<sub>2</sub> adduct, [Ru( $\eta^5$ -indenyl)(PAR<sub>2</sub>)( $\eta^2$ -H<sub>2</sub>)(PPh<sub>3</sub>)], in the formation of [RuH( $\eta^5$ -indenyl)(HPMe<sub>2</sub>)(PMe<sub>3</sub>)], a further indication of the importance of the variable binding modes of the terminal phosphido ligand in this system.



## INTRODUCTION

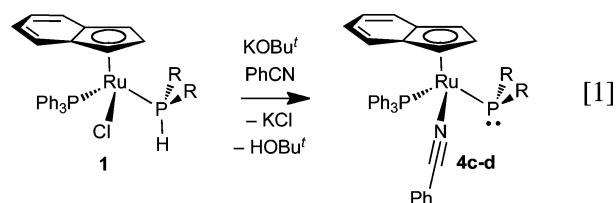
In our exploration of the coordination chemistry of secondary phosphines, we have prepared unusual five-coordinate phosphido complexes via the dehydrohalogenation reaction illustrated in Scheme 1.<sup>1a</sup> These dark blue complexes exhibit

Scheme 1



Ru=PR<sub>2</sub>  $\pi$  bonding and undergo a range of facile 1,2-addition chemistry, for both polar and nonpolar addenda,<sup>1a,b</sup> and [2 + 2]-cycloaddition reactions of both alkenes<sup>1c</sup> and alkynes,<sup>1d</sup> which are of particular interest in the development of new

catalysts for hydrophosphination.<sup>2</sup> So far, we have been able to isolate these very reactive complexes only for bulky alkyl substituents at phosphorus (R = Cy (2a), Pr<sup>i</sup> (2b)). We have identified the analogous diaryl species (R = Ph (2c), Tol<sup>p</sup> (2d)) at low temperature in solution by <sup>31</sup>P{<sup>1</sup>H} NMR, but these complexes decompose to a mixture of unidentified products as they are warmed to room temperature. We have also trapped the diarylphosphido complexes as their CO adducts (3c,d in Scheme 1);<sup>1a</sup> however, preliminary reactivity and photolysis studies<sup>3</sup> indicated that none of the carbonyl ligands in 3a–d is sufficiently labile to yield a reactive five-coordinate species able to participate in 1,2-addition or [2 + 2]-cycloaddition chemistry. We report here the synthesis and isolation of the corresponding benzonitrile adducts (4c,d, eq 1), from which



the benzonitrile ligands dissociate with relative ease. We also present a survey of the reactivity of both the carbonyl and

Received: September 1, 2011

Published: November 7, 2011



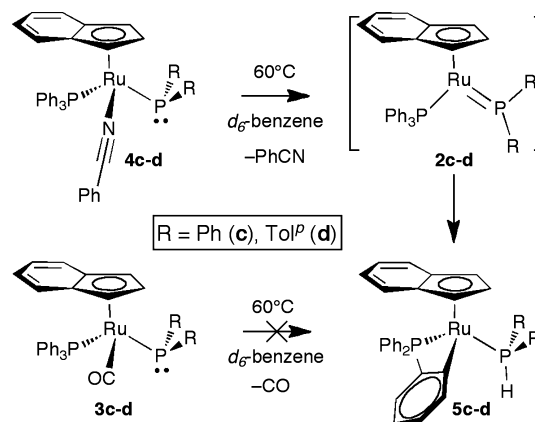
**Table 2. Crystallographic Data for  $[(\eta^5\text{-indenyl})\text{Ru}(\text{NCPH})(\text{PPh}_2)(\text{PPh}_3)]$  (**4c**)**

formula	$\text{C}_{46}\text{H}_{37}\text{NP}_2\text{Ru}$
formula wt	766.78
cryst color, habit	orange rod
cryst dimens (mm)	$0.10 \times 0.12 \times 0.46$
cryst syst, space group	orthorhombic, <i>Pbcn</i> (No. 60)
<i>a</i> (Å)	19.9629(6)
<i>b</i> (Å)	19.0706(6)
<i>c</i> (Å)	19.6393(6)
<i>V</i> (Å <sup>3</sup> )	7476.8(4)
<i>Z</i>	8
$\rho_{\text{calcd}}$ (g cm <sup>-3</sup> )	1.362
$\mu$ (mm <sup>-1</sup> )	0.538
temp (°C)	-100
data collection $2\theta_{\text{max}}$ (deg)	52.80
total no. of data collected	57 326 ( $-24 \leq h \leq 24$ , $-23 \leq k \leq 23$ , $-24 \leq l \leq 24$ )
no. of indep rflns ( $R_{\text{int}}$ )	7675 (0.0595)
no. of obsd rflns ( $F_o^2 \geq 2\sigma(F_o^2)$ )	5918
range of transmissn factors	0.9496–0.7883
no. of data/restraints/params	7675/0/451
goodness of fit ( <i>S</i> ) (all data) <sup>a</sup>	1.024
$R1$ ( $F_o^2 \geq 2\sigma(F_o^2)$ ) <sup>b</sup>	0.0293
wR2 (all data) <sup>c</sup>	0.0705
largest diff peak, hole (e Å <sup>-3</sup> )	0.312, -0.499

<sup>a</sup> $S = [\sum w(F_o^2 - F_c^2)^2 / (n - p)]^{1/2}$  (*n* = number of data; *p* = number of parameters varied;  $w = [\sigma^2(F_o^2) + (0.0247P)^2 + 6.0877P]^{-1}$ , where  $P = [\text{Max}(F_o^2, 0) + 2F_c^2]/3$ ). <sup>b</sup> $R1 = \sum |F_o| - |F_c| / \sum |F_o|$ . <sup>c</sup>wR2 =  $[\sum w(F_o^2 - F_c^2)^2 / \sum w(F_o^4)]^{1/2}$ .

presence of coordinated benzonitrile, with  $\nu_{\text{CN}}$  at 2199 cm<sup>-1</sup>. However, attempts to characterize this sample by solution NMR inevitably resulted in decomposition, including dissociation of the benzonitrile ligand and regeneration of **2b**, accompanied by thermal degradation to the orthometalated product **5b**<sup>1a</sup> (vide infra). It is not yet clear whether the greater stability of the diarylphosphido benzonitrile adducts **4c,d** in solution, relative to the dialkylphosphido analogues **4a,b**, is due to the lesser bulk of the diaryl-substituted phosphido ligands in **4c,d** or to their diminished donor ability.

Complexes **4c,d** are sufficiently stable to allow their isolation and characterization, but they are highly air-sensitive even in the solid state<sup>12</sup> and, in the absence of air or moisture, they undergo thermal decomposition in solution. Heating sealed samples of **4c,d** in *d*<sub>6</sub>-benzene to 60 °C gives a slow color change from deep purple-red to a clear orange-red, corresponding to the formation of the orthometalated products  $[\text{Ru}(\eta^5\text{-indenyl})\{\kappa^2\text{-}(o\text{-C}_6\text{H}_4)\text{PPh}_2\}(\text{PR}_2\text{H})]$  (**5c,d** in Scheme 2), as determined by <sup>31</sup>P{<sup>1</sup>H} NMR spectroscopy. Similarly to the previously characterized complexes **5a,b**,<sup>1a</sup> the <sup>31</sup>P{<sup>1</sup>H} signals for the orthometalated PPh<sub>3</sub> ligand in **5c,d** show a diagnostic upfield shift, from ~52 ppm in **4c,d** to -18.7 ppm (**5c**) and -18.5 ppm (**5d**). <sup>31</sup>P NMR confirms the presence of the secondary phosphine ligands in **5c,d**: signals at 46.5 and 44.6 ppm, respectively, show a large <sup>1</sup>J<sub>PH</sub> value of 342 Hz, and similar coupling constants are observed for the P-H signals in the corresponding <sup>1</sup>H NMR spectra. In contrast, samples of the carbonyl adducts **3c,d** in *d*<sub>8</sub>-toluene are quite

**Scheme 2**

stable to thermal decomposition, showing no change by <sup>31</sup>P{<sup>1</sup>H} NMR even with prolonged heating (5 days) at 60 °C. This is consistent with the higher  $\pi$  acidity of CO relative to that of benzonitrile, which leads to stronger M-L bonds in these electron-rich ruthenium complexes. Computed ligand dissociation enthalpies (Table 3) for the conversion of **3a-d** to **2a-d** plus CO and for **4a-d** to **2a-d** plus NCPH, respectively, indicate that CO binds approximately twice as strongly as benzonitrile to Ru throughout this series. The calculated Ru-CO dissociation enthalpies for the dialkylphosphido complexes **3a,b** are similar to experimental CO dissociation energies of 41–44 kcal/mol reported for Ru(CO)<sub>5</sub>, Ru<sub>3</sub>(CO)<sub>12</sub>, and Ru(dmpe)<sub>2</sub>CO.<sup>13</sup> We have found no absolute bond dissociation data for ruthenium (or other) nitrile complexes, but our calculated Ru-NCPH values are close to those determined by solution calorimetry for Ru-PR<sub>3</sub> bonds in half-sandwich complexes, which fall in the range of 9–24 kcal/mol.<sup>14</sup> Most striking is the approximately 7 kcal/mol increase in calculated ligand dissociation enthalpies for the diarylphosphido complexes **3c,d** and **4c,d** relative to the corresponding dialkylphosphido complexes **3a,b** and **4a,b**, consistent with our observation of the instability of **4b** relative to **4c,d** (vide supra).

**Table 3. Computed Ligand Dissociation Enthalpies  $\Delta H$  (kcal mol<sup>-1</sup>)<sup>a</sup>**

R	L = CO (3)	L = PhCN (4)
Cy (a)	45.4	18.1
Pr (b)	45.1	17.9
Ph (c)	52.0	24.6
TolP (d)	52.3	25.3

<sup>a</sup>PBE/DKH2-TZVP calculations.

The fact that complexes **4c,d** give the same thermal decomposition product as the five-coordinate dialkylphosphido complexes **2a,b** suggests that these adducts cleanly dissociate benzonitrile to generate the diarylphosphido complexes **2c,d** in solution. This is further supported by addition of dihydrogen to the adducts in *d*<sub>6</sub>-benzene, which generates the secondary

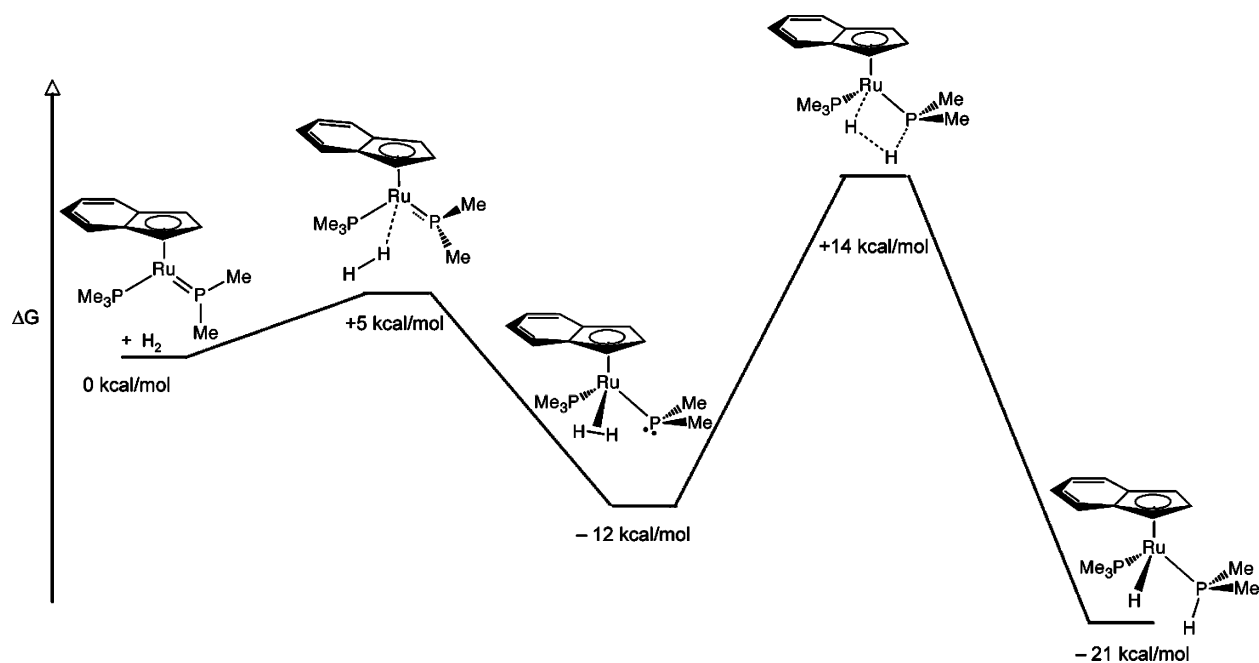
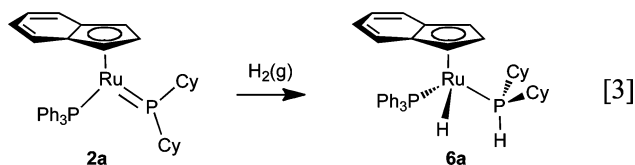
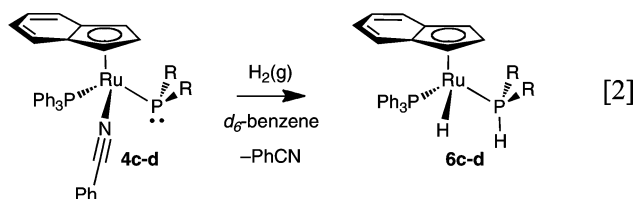


**Figure 2.** PBE/DKH2-TZVP free energy reaction profile for a simplified model ( $\text{PPh}_3$  replaced by  $\text{PMe}_3$ ; Cy or  $\text{Pr}^i$  replaced by Me) of the addition of  $\text{H}_2$  to **2a,b**.

phosphine hydrido complexes  $[\text{RuH}(\eta^5\text{-indenyl})(\text{PR}_2\text{H})(\text{PPh}_3)]$  (**6c,d**) within seconds (eq 2), on the basis of the

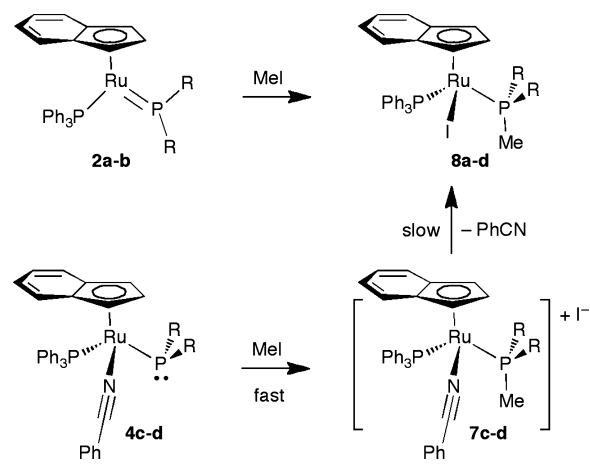


color change from deep purple-red to clear yellow-orange, and as confirmed by  $^1\text{H}$  and  $^{31}\text{P}\{^1\text{H}\}$  NMR.<sup>15</sup> The same overall 1,2-addition product **6a** results from the addition of  $\text{H}_2(\text{g})$  to complex **2a** (eq 3),<sup>1a</sup> and similar hydrido amine or phosphine complexes have resulted from the addition of dihydrogen to other metal amido or phosphido complexes, respectively.<sup>16</sup> This apparent outer-sphere activation of dihydrogen is analogous to that proposed to occur for the Noyori-type ruthenium amide hydrogenation catalysts.<sup>17</sup> We have put some effort into identifying the trajectory of hydrogen addition, computationally, to better understand this process. DFT results for a simplified dialkylphosphido ruthenium indenyl complex are shown in Figure 2. The intermediate  $\eta^2\text{-H}_2$  adduct highlights the importance to this reaction of the ready access to coordinative unsaturation at Ru resulting from disruption of the Ru–P double bond.<sup>18</sup> Although the overall reaction is formally a heterolytic cleavage of dihydrogen, the hydrogens in the  $\eta^2$  adduct carry zero charge, and in the cyclic transition

state, the H on Ru has a calculated charge of  $-0.1$ , while the H on P has a charge of  $+0.1$ , a very small charge separation. It is easy to visualize the ready dissociative substitution of benzonitrile by dihydrogen as an entry to this essentially homolytic pathway of addition across the  $\text{Ru}=\text{PAr}_2$  bond in **4c,d**.

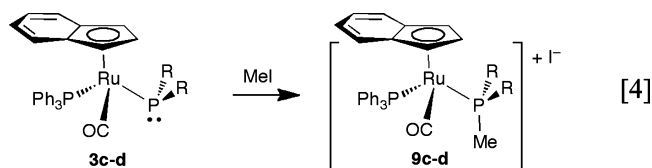
We showed previously that the dialkylphosphido complexes **2a,b** undergo 1,2-addition of the polar bonds in reagents such as HCl and methyl iodide,<sup>1a</sup> as well as a range of protic reagents.<sup>1b</sup> As shown for methyl iodide in Scheme 3, these reactions invariably place the electrophilic portion of the addendum at P and the nucleophilic portion at the coordinatively unsaturated Ru. Addition of MeI to the benzonitrile adducts **4c,d** ultimately gives the analogous diarylmethylphosphine iodide complexes **8c,d** (Scheme 3),

**Scheme 3**



but our studies of this reaction indicate a stepwise mechanism in which nucleophilic attack of the terminal phosphido ligand at

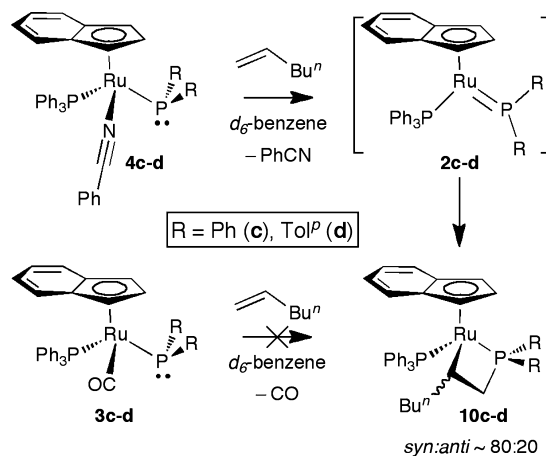
$\text{Me}^{\delta+}$  generates the cationic intermediate **7**, which then undergoes nucleophilic substitution of the benzonitrile at Ru by  $\text{I}^-$ . The addition of MeI to **4c,d** in toluene results in the immediate formation of a bright yellow precipitate (1–2 s), which, when dissolved in *d*-chloroform, slowly converts from clear yellow to clear orange-red. The identity of the yellow precipitate as  $[\text{Ru}(\eta^5\text{-indenyl})(\text{NCPh})(\text{PPh}_3)(\text{PR}_2\text{Me})]\text{I}$  (**7c,d**) was confirmed by observation of  $\nu_{\text{CN}}$  ( $2239\text{ cm}^{-1}$ , **7c**;  $2227\text{ cm}^{-1}$ , **7d**) in the IR spectra and observation of the cation mass peaks by ESI-MS, with predicted isotopic distributions (see the Supporting Information).  $^1\text{H}$  NMR spectra show a diagnostic doublet with  $^2J_{\text{PH}} = 9\text{ Hz}$  at 1.2–1.3 ppm due to the new P–CH<sub>3</sub> group.  $^{31}\text{P}\{^1\text{H}\}$  NMR spectra of these *d*-chloroform solutions initially show major signals due to the benzonitrile adducts **7c,d**, but we also see small signals due to  $[\text{Ru}(\eta^5\text{-indenyl})(\text{PPh}_3)(\text{PR}_2\text{Me})]$  (**8c,d**).<sup>19</sup> These gradually increase in intensity (over 5 days) to become the major product signals. In the  $^1\text{H}$  NMR spectra the P–Me signals remain but shift slightly ( $\sim 0.5\text{ ppm}$ ).<sup>20</sup> Cationic complexes analogous to the benzonitrile-containing **7c,d**,  $[\text{Ru}(\eta^5\text{-indenyl})(\text{CO})(\text{PPh}_3)(\text{PR}_2\text{Me})]\text{I}$  (**9c,d**), result from the addition of excess MeI to the carbonyl complexes **3c,d** (eq 4), again as diagnosed by  $^1\text{H}$  NMR, IR, and



ESI-MS. These carbonyl cations are stable in *d*-chloroform indefinitely at room temperature, showing no sign of substitution of the CO ligand by the  $\text{I}^-$  counterion.

As described in the Introduction, the dialkylphosphido complexes **2a,b** participate in [2 + 2]-cycloaddition reactions with alkenes and alkynes.<sup>1c,d</sup> Of particular note is the fact that even the simple olefins ethylene and 1-hexene participate in this apparently concerted cycloaddition. Our final test of the ability of **4c,d** to act as masked sources of the coordinatively unsaturated **2c,d** involved the addition of 1-hexene to these benzonitrile adducts. We screened the behavior of both **3c,d** and **4c,d** in the presence of an excess of 1-hexene, in sealed NMR tube experiments. The carbonyl adducts **3c,d** showed no reaction with the alkene, while the benzonitrile adducts **4c,d** gradually changed color from dark purple-red to red-orange, and  $^{31}\text{P}\{^1\text{H}\}$  NMR showed that first one and then a second, minor product formed, with signals corresponding closely in shift and  $^2J_{\text{PP}}$  values to those previously observed for the syn and anti diastereomers of the [2 + 2]-cycloadducts  $[\text{Ru}(\eta^5\text{-indenyl})(\kappa^2\text{-Bu}^n\text{CH}_2\text{CH}_2\text{PR}_2)(\text{PPh}_3)]$  (**10a,b**).<sup>1c</sup> The high-field signals ( $-19.3$  to  $-23.2\text{ ppm}$ ) are particularly diagnostic of the incorporation of “ $\text{PR}_2$ ” into the four-membered metallacycle. We presume that the cycloaddition of 1-hexene at **4c,d** is proceeding with similar regiochemistry to give the analogous syn and anti diastereomers of **10c,d**, where syn and anti refer to the orientation of the  $\text{Bu}^n$  substituent on the  $\alpha$ -carbon with respect to the Ru–indenyl bond (Scheme 4). Upon complete consumption of **4c,d** in these reactions the diastereomer ratio (by analogy to assignments for **10a,b**) is about 80:20 syn/anti, which is slightly lower than the  $>95:5$  ratio observed for **10a,b**. Interestingly, a second set of sealed NMR tube experiments, in which slightly less than 1 equiv of 1-hexene was added to **4c,d**, gave only the putative syn diastereomers as products, with trace

Scheme 4



amounts of the anti products appearing only after 1 day or more. This surprising difference in the 1-hexene concentration dependences of the formation of the two diastereomers is not out of line with our ongoing studies of the cycloaddition reactions of 1-hexene at **2a,b**, for which we observe a kinetic preference for the formation of the syn isomer, facile cycloreversion, and slow epimerization.<sup>21</sup>

## CONCLUSIONS

With the synthesis of these benzonitrile-stabilized terminal diarylphosphido complexes, we have expanded the scope of a series of highly reactive five-coordinate ruthenium half-sandwich fragments. The reactivity and computational studies described above illustrate the importance of ready access to a vacant coordination site at ruthenium, via facile ligand dissociation or variable phosphido binding mode, to allow the addition of nonpolar H–H or C–H bonds, or [2 + 2]-cycloaddition of alkenes, at the Ru– $\text{PR}_2$  bond. Meanwhile, the stepwise reactions with MeI confirm that the nucleophilicity at the terminal phosphido ligands in these complexes is not compromised by the presence of less donating aryl substituents at P or by the ready dissociation of the benzonitrile ligands. We are currently studying the mechanism(s) of cycloaddition in these complexes more closely and examining their activity in catalytic phosphination and hydrophosphination reactions.

## EXPERIMENTAL SECTION

**General Considerations.** Unless otherwise noted, all reactions and manipulations were performed under nitrogen in an MBraun Unilab 1200/780 glovebox or using conventional Schlenk techniques. All solvents were sparged with nitrogen for 25 min and dried using an MBraun Solvent Purification System (SPS). Deuterated solvents were purchased from Canadian Isotopes Laboratory (CIL), freeze–pump–thaw-degassed, and vacuum-transferred from sodium/benzophenone (*d*<sub>6</sub>-benzene, *d*<sub>8</sub>-toluene) calcium hydride (*d*-chloroform) before use. Benzonitrile was predried with  $\text{K}_2\text{CO}_3$  and fractionally distilled from  $\text{P}_2\text{O}_5$  under dynamic vacuum. Potassium *tert*-butoxide was purchased from Aldrich Chemical Co. and used as received without further purification. Carbon monoxide and hydrogen gas were purchased from Praxair Canada Inc.  $[\text{Ru}(\eta^5\text{-indenyl})\text{Cl}(\text{PR}_2\text{H})(\text{PPh}_3)]$  ( $\text{R} = \text{Ph}$  (**1c**<sup>6</sup>),  $\text{To}^p$  (**1d**<sup>1a</sup>)),  $[\text{Ru}(\eta^5\text{-indenyl})(\text{PPh}_3)(\text{PR}_2)]$  (**2b**<sup>1a</sup>), and  $[\text{Ru}(\eta^5\text{-indenyl})(\text{CO})(\text{PR}_2)(\text{PPh}_3)]$  ( $\text{R} = \text{Ph}$  (**3c**),  $\text{To}^p$  (**3d**))<sup>1a</sup> were prepared as previously reported in the literature. (All secondary phosphines were purchased from Strem Chemicals as 10 wt % solutions in hexanes; concentrations were checked against a known quantity of triphenylphosphine oxide by  $^{31}\text{P}\{^1\text{H}\}$  NMR before use.)

$^{31}\text{P}$  NMR data are given in Table 1.  $^1\text{H}$  and  $^{13}\text{C}$  NMR data for **4c,d** and  $^1\text{H}$  NMR data for products of the NMR scale reactions are in the Supporting Information. NMR spectra were recorded on a Bruker AVANCE 500 operating at 500.13 MHz for  $^1\text{H}$ , 125.77 MHz for  $^{13}\text{C}$ , and 202.46 MHz for  $^{31}\text{P}$  or on a Bruker AVANCE 300 operating at 300.13 MHz for  $^1\text{H}$ , 74.47 MHz for  $^{13}\text{C}$ , and 121.49 MHz for  $^{31}\text{P}$ . Chemical shifts are reported in ppm at ambient temperature unless otherwise noted.  $^1\text{H}$  chemical shifts are referenced against residual protonated solvent peaks at 7.16 ( $\text{C}_6\text{D}_6$ ), 2.09 ( $\text{PhCD}_2\text{H}$ ), and 7.26 ppm ( $\text{CHCl}_3$ ).  $^{13}\text{C}$  chemical shifts are referenced against  $d_6$ -benzene at 128.4 ppm and  $d_8$ -toluene at 20.4 ppm. All  $^1\text{H}$  and  $^{13}\text{C}$  chemical shifts are reported relative to tetramethylsilane, and  $^{31}\text{P}$  chemical shifts are reported relative to 85%  $\text{H}_3\text{PO}_4(\text{aq})$ .

IR spectra were recorded for KBr pellets under a nitrogen atmosphere on a Perkin-Elmer FTIR Spectrum One spectrometer. UV-vis data were obtained using a Varian Cary 5 UV-vis spectrophotometer. Microanalysis was performed by Canadian Microanalytical Service Ltd., Delta, BC, Canada. Low-resolution mass spectra were collected at the University of Victoria on a Micromass Q-ToF micro hybrid quadrupole/time-of-flight mass spectrometer in positive-ion mode using electrospray ionization. High-resolution mass spectra were acquired by Dr. Yun Ling at the University of British Columbia, Vancouver, BC, Canada, on a Water/Micromass LCT-ToF mass spectrometer in positive-ion mode using electrospray ionization.

**Synthesis of Benzonitrile Adducts 4c,d.**  $[\text{Ru}(\eta^5\text{-indenyl})(\text{PPh}_2)(\text{PhCN})(\text{PPh}_3)]$  (**4c**). To a Schlenk flask containing  $[\text{Ru}(\eta^5\text{-indenyl})\text{Cl}(\text{HPPH}_2)(\text{PPh}_3)]$  (**1c**; 423 mg, 0.604 mmol) and  $\text{KOBU}^t$  (132 mg, 1.18 mmol) was added benzonitrile (0.31 mL, 0.31 g, 3.0 mmol) to form a dark red sludge. Toluene (25 mL) was added, and the resulting purple-red mixture was stirred for 3 h, after which it was filtered through Celite to remove solid and gelatinous byproducts  $\text{KCl}$  and  $\text{HOBu}^t$ . The toluene was removed under vacuum, and the resulting red paste was precipitated from a minimum volume of toluene (3 mL) layered with pentane (25 mL). The dark red powder was then washed with pentane ( $4 \times 10$  mL) to give  $[\text{Ru}(\eta^5\text{-indenyl})(\text{PhCN})(\text{PPh}_2)(\text{PPh}_3)]$  (**4c**; 272 mg, 0.355 mmol, 59% yield). IR (KBr,  $\text{cm}^{-1}$ ): 2198 (s,  $\nu_{\text{CN}}$ ). UV-vis (toluene):  $\lambda_{\text{max}}$  523 nm,  $\epsilon$  3000  $\text{M}^{-1} \text{cm}^{-1}$ . HR-ESI-MS ( $[\text{M} + \text{H}]^+$ ,  $m/z$ ): calcd for  $\text{C}_{46}\text{H}_{38}\text{NP}_2^{99}\text{Ru}$  765.1539, found 765.1558 (error 2.5 ppm). Anal. Calcd for  $\text{C}_{46}\text{H}_{37}\text{NP}_2\text{Ru}$ : C, 72.03; H, 4.87. Found: C, 71.99; H, 4.93. Dec pt: 148–150 °C.

$[\text{Ru}(\eta^5\text{-indenyl})(\text{PTolP}_2)(\text{PhCN})(\text{PPh}_3)]$  (**4d**). This complex was prepared by a method similar to that for **4c**, using  $[\text{Ru}(\eta^5\text{-indenyl})\text{Cl}(\text{HPTolP}_2)(\text{PPh}_3)]$  (**1d**; 270 mg, 0.371 mmol),  $\text{KOBU}^t$  (84 mg, 0.75 mmol), and benzonitrile (0.21 mL, 0.21 g, 2.0 mmol). The product  $[\text{Ru}(\eta^5\text{-indenyl})(\text{PhCN})(\text{PTolP}_2)(\text{PPh}_3)]$  (**4d**) was isolated as a dark red powder (188 mg, 0.237 mmol, 64% yield). IR (KBr,  $\text{cm}^{-1}$ ): 2198 (s,  $\nu_{\text{CN}}$ ). UV-vis (toluene):  $\lambda_{\text{max}}$  523 nm,  $\epsilon$  3000  $\text{M}^{-1} \text{cm}^{-1}$ . HR-ESI-MS ( $[\text{M} + \text{H}]^+$ ,  $m/z$ ): calcd for  $\text{C}_{48}\text{H}_{42}\text{NP}_2^{99}\text{Ru}$  793.1852, found 793.1827 (error -3.1 ppm). High air sensitivity precluded the satisfactory elemental analysis of this complex (see the Supporting Information for  $^1\text{H}$  and  $^{31}\text{P}\{^1\text{H}\}$  spectra of isolated product). Dec pt: 148–150 °C.

**Attempted Isolation of  $[\text{Ru}(\eta^5\text{-indenyl})(\text{PPr}^t_2)(\text{PhCN})(\text{PPh}_3)]$  (**4b**).** To a Schlenk flask containing  $[\text{Ru}(\text{PPr}^t_2)(\eta^5\text{-indenyl})(\text{PPh}_3)]$  (**2b**; 82 mg, 0.14 mmol) in toluene (5 mL) was added an excess of benzonitrile (720 mg, 7 mmol, ~50 equiv), which caused the dark blue solution to turn deep red. The mixture was stirred for approximately 10 min, and then the solvent was removed under vacuum. Trituration of the resulting bright red oily residue with pentane ( $4 \times 5$  mL) gave a tacky reddish solid (crude yield 79 mg, 0.11 mmol, 81%). IR (KBr pellet,  $\text{cm}^{-1}$ ): 2199 (w,  $\nu_{\text{CN}}$ ).

**NMR-Scale Reactions of the Adducts  $[\text{Ru}(\eta^5\text{-indenyl})(\text{PR}_2)(\text{L})(\text{PPh}_3)]$  ( $\text{L} = \text{CO}$  (**3c,d**),  $\text{PhCN}$  (**4c,d**)).** (a). *Thermolysis.* Solid  $[\text{Ru}(\eta^5\text{-indenyl})(\text{CO})(\text{PR}_2)(\text{PPh}_3)]$  (**3c**, 6 mg, 0.008 mmol; **3d**, 5 mg, 0.006 mmol) or  $[\text{Ru}(\eta^5\text{-indenyl})(\text{PhCN})(\text{PR}_2)(\text{PPh}_3)]$  (**4c**, 5 mg, 0.007 mmol; **4d**, 8 mg, 0.011 mmol) was dissolved in  $d_8$ -toluene (**3c,d**, 0.7 mL) or  $d_6$ -benzene (**4c,d**, 0.7 mL) and added to a J. Young NMR tube. The NMR sample was heated to 60 °C in an oil bath and was removed periodically for monitoring by  $^{31}\text{P}\{^1\text{H}\}$  NMR spectroscopy.

For **3c,d**, samples remained dark red, and initial  $^{31}\text{P}\{^1\text{H}\}$  spectra showed no changes. After 5 days,  $^{31}\text{P}\{^1\text{H}\}$  spectra still showed principally unreacted **3c,d**, along with small amounts of  $\text{PPh}_3$  (<5%) and an unidentified product (in **3c**, singlet at -56.7 ppm (<5%); in **3d**, singlet at -58.9 ppm (<5%).

For **4c,d**, samples gradually (**4c**, 90 h; **4d**, 70 h) lightened from deep purple-red to clear orange-red, at which point  $^{31}\text{P}\{^1\text{H}\}$  NMR showed conversion to the orthometalated complexes  $[\text{Ru}(\eta^5\text{-indenyl})\{\kappa^2\text{-}(o\text{-C}_6\text{H}_4)\text{PPh}_2\}(\text{PR}_2\text{H})]$  (**5c,d**), by analogy to shifts and coupling constants previously observed for the orthometalated dialkylphosphine complex **5a**<sup>1a</sup>.

(b). *Reaction with  $\text{H}_2(\text{g})$ .* Solid  $[\text{Ru}(\eta^5\text{-indenyl})(\text{CO})(\text{PR}_2)(\text{PPh}_3)]$  (**3c**, 5 mg, 0.007 mmol; **3d**, 5 mg, 0.006 mmol) or  $[\text{Ru}(\eta^5\text{-indenyl})(\text{PhCN})(\text{PR}_2)(\text{PPh}_3)]$  (**4c**, 5 mg, 0.007 mmol; **4d**, 5 mg, 0.007 mmol) was dissolved in  $d_6$ -benzene (**3c**, **4d**, 0.6 mL) or  $d_8$ -toluene (**3d**, **4c**, 0.6 mL) and added to a J. Young NMR tube. The sample was degassed by three freeze-pump-thaw cycles before approximately 1 atm of hydrogen was introduced. The sealed sample was inverted five times, and the contents were then analyzed by  $^{31}\text{P}\{^1\text{H}\}$  NMR spectroscopy.

For **3c,d**, samples retained their red color, and  $^{31}\text{P}\{^1\text{H}\}$  spectra showed no changes.

For **4c,d**, the dark purple-red solutions turned clear yellow-orange after the sample was inverted (~10 s), and  $^{31}\text{P}\{^1\text{H}\}$  NMR showed complete conversion to the hydrido phosphine complexes  $[\text{Ru}(\eta^5\text{-indenyl})(\text{H})(\text{PR}_2)(\text{PPh}_3)]$  (**6c,d**).<sup>13</sup>

(c). *Reaction with MeI.* Solid  $[\text{Ru}(\eta^5\text{-indenyl})(\text{CO})(\text{PR}_2)(\text{PPh}_3)]$  (**3c**, 28 mg, 0.040 mmol; **3d**, 25 mg, 0.035 mmol) or  $[\text{Ru}(\eta^5\text{-indenyl})(\text{NCPh})(\text{PR}_2)(\text{PPh}_3)]$  (**4c**, 37 mg, 0.046 mmol; **4d**, 30 mg, 0.038 mmol) was dissolved in toluene (1–5 mL). MeI (50  $\mu\text{L}$ , 0.8 mmol) was added to the dark red solutions.

For **3c,d**, mixtures immediately formed a yellow precipitate along with a solution color change to clear yellow (1–2 s). Toluene was removed under vacuum, and analysis of the resulting yellow precipitates by NMR, IR, and ESI-MS indicated they were the iodide salts  $[\text{Ru}(\eta^5\text{-indenyl})(\text{CO})(\text{PR}_2\text{Me})(\text{PPh}_3)]\text{I}$  (**9c,d**).  $^{31}\text{P}\{^1\text{H}\}$  NMR spectra of the samples in  $d$ -chloroform showed that **9c,d** was the major product, although there were minor P-containing impurities. Continued monitoring of these clear yellow samples by  $^{31}\text{P}\{^1\text{H}\}$  NMR showed no changes over 3–5 days.

Data for **9c**: LR-ESI-MS (20 V,  $\text{CH}_2\text{Cl}_2$ ,  $m/z$ ) 707.2 ( $\text{M}^+$ , 100%); IR (KBr,  $\text{cm}^{-1}$ ) 1959 (s,  $\nu_{\text{CO}}$ ).

Data for **9d**: LR-ESI-MS (20 V,  $\text{CH}_2\text{Cl}_2$ ,  $m/z$ ) 735.2 ( $\text{M}^+$ , 100%); IR (KBr,  $\text{cm}^{-1}$ ) 1980 (s,  $\nu_{\text{CO}}$ ).

For **4c,d**, mixtures formed a yellow precipitate within 1–2 s, with light orange supernatant solutions. Toluene was removed under vacuum, and analysis of the resulting yellow precipitates by NMR, IR, and ESI-MS indicated they were the iodide salts  $[\text{Ru}(\eta^5\text{-indenyl})(\text{NCPh})(\text{PR}_2\text{Me})(\text{PPh}_3)]\text{I}$  (**7c,d**). The NMR samples in  $d$ -chloroform slowly darkened from yellow-orange to red-orange. Continued monitoring by  $^{31}\text{P}\{^1\text{H}\}$  NMR showed complete consumption of **7c,d** after 11 days, at which point **8c,d** were the major products in solution.

Data for **7c**: LR-ESI-MS (20 V,  $\text{CH}_2\text{Cl}_2$ ,  $m/z$ ) 782.1 ( $\text{M}^+$ , 50%), 679.0 ( $[\text{M} - \text{PhCN}]^+$ , 100%); IR (KBr,  $\text{cm}^{-1}$ ) 2239 (s,  $\nu_{\text{CN}}$ ).

Data for **7d**: ESI-MS (20 V,  $\text{CH}_2\text{Cl}_2$ ,  $m/z$ ) 810.2 ( $\text{M}^+$ , 40%), 707.1 ( $[\text{M} - \text{PhCN}]^+$ , 100%); IR (KBr,  $\text{cm}^{-1}$ ) 2227 (s,  $\nu_{\text{CN}}$ ).

(d). *Reaction with Excess 1-Hexene.* Solid  $[\text{Ru}(\eta^5\text{-indenyl})(\text{CO})(\text{PR}_2)(\text{PPh}_3)]$  (**3c**, 7 mg, 0.01 mmol; **3d**, 7 mg, 0.01 mmol) or  $[\text{Ru}(\eta^5\text{-indenyl})(\text{PhCN})(\text{PR}_2)(\text{PPh}_3)]$  (**4c**, 8 mg, 0.01 mmol; **4d**, 8 mg, 0.01 mmol) was dissolved in  $d_6$ -benzene (1.0 mL) and added to a sealable NMR tube. The sample was freeze-pump-thaw-degassed three times. 1-Hexene (0.10 mL, 0.81 mmol) was added by syringe, and the tube was flame-sealed. The thawed sample was inverted five times to mix the reagents and then monitored by  $^{31}\text{P}\{^1\text{H}\}$  NMR spectroscopy.

For **3c,d**, samples remained dark red, and  $^{31}\text{P}\{^1\text{H}\}$  NMR spectra showed no changes, even after 24 h.

For **4c,d**, both dark red samples gradually changed to clear red-orange (18–21 h).

(e). *Reaction with 1 equiv of 1-Hexene.* Solid  $[\text{Ru}(\eta^5\text{-indenyl})\text{-}(\text{PhCN})(\text{PR}_2)(\text{PPh}_3)]$  (**4c**, 10 mg, 0.013 mmol; **4d**, 10 mg, 0.013 mmol) was dissolved in *d*<sub>6</sub>-benzene (0.7 mL) and added to a sealable NMR tube. 1-Hexene (0.161 M in toluene, 0.08 mL, 0.01 mmol) was added by syringe, and the tube was flame-sealed. The sample was inverted five times to mix the reagents and then monitored by  $^{31}\text{P}\{^1\text{H}\}$  NMR spectroscopy.

For **4c,d**, for both samples, the dark red color persisted over several days, despite changes in the  $^{31}\text{P}\{^1\text{H}\}$  NMR spectra, due to the presence of residual, darkly colored starting material. ( $^1\text{H}$  NMR confirmed the complete consumption of 1-hexene.)

**X-ray Structure Determination.** Crystals of **4c** were grown via slow diffusion of hexanes into a toluene solution of the compound. Data were collected using Mo  $K\alpha$  radiation ( $\lambda = 0.71073 \text{ \AA}$ ) on a Bruker APEX II CCD detector/PLATFORM diffractometer<sup>22</sup> with the crystals cooled to  $-100 \text{ }^\circ\text{C}$ . The data were corrected for absorption through Gaussian integration from indexing of the crystal faces. The structure was solved using a Patterson search for heavy atoms followed by structure expansion (DIRDIF-2008<sup>23</sup>). Refinements were completed using full-matrix least squares on  $F^2$  (SHELXL-97<sup>24</sup>). All non-hydrogen atoms were refined with anisotropic displacement parameters. All hydrogen atoms were assigned positions based on the idealized  $\text{sp}^2$  or  $\text{sp}^3$  geometries of their attached atoms and were given thermal parameters 20% greater than those of the parent carbons. Further crystallographic experimental data and refinement details can be found in Table 2.

**Computational Details.** For all calculations the Perdew–Burke–Ernzerhof density functional (PBE)<sup>25</sup> was employed. Scalar relativistic effects were explicitly treated using the second-order Douglas–Kroll–Hess Hamiltonian,<sup>26</sup> in combination with all-electron TZVP basis sets of the Karlsruhe group,<sup>27</sup> appropriately recontracted to satisfy the requirements of the scalar relativistic Hamiltonian.<sup>28</sup> The resolution of the identity approximation was used with decontracted auxiliary TZV/J basis sets. Harmonic vibrational frequencies and thermodynamic corrections were obtained at the same level of theory. All calculations were performed with the ORCA program<sup>29</sup> using tight convergence criteria and enhanced integration grids.

## ■ ASSOCIATED CONTENT

### ● Supporting Information

Tables and figures giving  $^1\text{H}$  and  $^{13}\text{C}\{^1\text{H}\}$  NMR data for **4c,d**,  $^1\text{H}$  NMR data for products of NMR scale reactions of **3c,d** and **4c,d**,  $^{31}\text{P}\{^1\text{H}\}$  NMR spectra of the progress of NMR scale reactions of **4c,d**, ESI-MS data for **7c,d** and **9c,d**, and Cartesian coordinates of all optimized structures and a CIF file giving crystallographic data for **4c**. This material is available free of charge via the Internet at <http://pubs.acs.org>.

## ■ AUTHOR INFORMATION

### Corresponding Author

\*E-mail: [lisarose@uvic.ca](mailto:lisarose@uvic.ca).

## ■ ACKNOWLEDGMENTS

We thank the Natural Sciences and Engineering Research Council (NSERC) of Canada for funding.

## ■ REFERENCES

- (1) (a) Derrah, E. J.; Pantazis, D. A.; McDonald, R.; Rosenberg, L. *Organometallics* **2007**, *26*, 1473. (b) Derrah, E. J.; Giesbrecht, K. E.; McDonald, R.; Rosenberg, L. *Organometallics* **2008**, *27*, 5025. (c) Derrah, E. J.; Pantazis, D. A.; McDonald, R.; Rosenberg, L. *Angew. Chem., Int. Ed.* **2010**, *49*, 3367. (d) Derrah, E. J.; McDonald, R.; Rosenberg, L. *Chem. Commun.* **2010**, *46*, 4592.
- (2) (a) Glueck, D. S. *Top. Organomet. Chem.* **2010**, *31*, 65. (b) Waterman, R. *Dalton Trans.* **2009**, 18.
- (3) Derrah, E. J. Ph.D. Thesis, University of Victoria, Victoria, 2009.
- (4)  $^{31}\text{P}\{^1\text{H}\}$  NMR of the crude reaction mixtures indicate complete consumption of **1c,d**. In some trials we see traces (<5%) of an unidentified impurity containing a single phosphorus environment (singlet at 36.2 ppm (R = Ph) or 36.5 ppm (R = Tol<sup>p</sup>)).
- (5) Similarly low  $^2J_{\text{PP}}$  values have been reported for other mixed  $\text{PR}_3/\text{pyramidal PR}'_2$  complexes: (a) Planas, J. G.; Gladysz, J. A. *Inorg. Chem.* **2002**, *41*, 6947. (b) Planas, J. G.; Hampel, F.; Gladysz, J. A. *Chem. Eur. J.* **2005**, *11*, 1402.
- (6) Derrah, E. J.; Marlinga, J. C.; Mitra, D.; Friesen, D. M.; Hall, S. A.; McDonald, R.; Rosenberg, L. *Organometallics* **2005**, *24*, 5817.
- (7) The relative  $^1\text{H}$  shifts and multiplicities for peaks due to the aromatic protons on coordinated benzonitrile are very similar to those we observe for free benzonitrile in *d*<sub>6</sub>-benzene: 7.11–6.97 (m,  $\text{H}_p$ ), 6.97–6.81 (m,  $\text{H}_o$ ), and 6.81–6.64 (m,  $\text{H}_m$ ) ppm.
- (8) Mrozek, M. F.; Wasileski, S. A.; Weaver, M. J. *J. Am. Chem. Soc.* **2001**, *123*, 12817.
- (9) Values of  $\nu_{\text{CN}}$  for transition-metal nitrile complexes are often higher than for the free nitrile: (a) Storhoff, B. N.; Lewis, H. C. *Coord. Chem. Rev.* **1977**, *23*, 1. (b) Kuznetsov, M. L.; Dement'ev, A. I.; Nazarov, A. A. *Russ. J. Inorg. Chem.* **2005**, *50*, 731. This can be rationalized by  $\sigma$  donation of the lone pair at N (which renders the N more electropositive and strengthens the N–C  $\sigma$ -bond) and the low  $\pi$  acidity of the N-bound nitrile (consider the sizes of the  $\pi^*$  lobes at N (small) and C (large), relative to coordinated CO). However, there are other examples of Ru(II) nitrile complexes that show red-shifted  $\nu_{\text{CN}}$  values similar to those of **4c,d**: (c) Ford, P. C. *Coord. Chem. Rev.* **1970**, *5*, 75. (d) Alves, J. J. F.; Franco, D. W. *Polyhedron* **1996**, *15*, 3299.
- (10) (a) Barre, C.; Boudot, P.; Kubicki, M. M.; Moise, C. *Inorg. Chem.* **1995**, *34*, 284. (b) Buhro, W. E.; Zwick, B. D.; Georgiou, S.; Hutchinson, J. P.; Gladysz, J. A. *J. Am. Chem. Soc.* **1988**, *110*, 2427.
- (11) Faller, J. W.; Crabtree, R. H.; Habib, A. *Organometallics* **1985**, *4*, 929. Typically a slip distortion of less than 0.25  $\text{\AA}$  indicates  $\eta^5$ -indenyl coordination.
- (12) The deep red-purple solids turn light orange-brown within seconds upon exposure to air.
- (13)  $\text{Ru}(\text{CO})_5$ : (a) Behrens, R.G. *J. Less-Common Met.* **1977**, *56*, 55.  $\text{Ru}_3(\text{CO})_{12}$ : (b) Connor, J.; et al. *Top. Current Chem.* **1977**, *71*, 71. (c) Housecroft, C. E.; Wade, K.; Smith, B. C. *J. Chem. Soc., Chem. Commun.* **1978**, 765.  $\text{Ru}(\text{dmpe})_2\text{CO}$ : (d) Belt, S. T.; Scaiano, J. C.; Whittlesey, M. K. *J. Am. Chem. Soc.* **1993**, *115*, 1921.
- (14) Luo, L.; Zhu, N.; Zhu, N. J.; Stevens, E. D.; Nolan, S. P.; Fagan, P. J. *Organometallics* **1994**, *13*, 669.
- (15) Complex **6c** was prepared previously by the addition of NaOMe to complex **1c**,<sup>6</sup> and complex **6b** was identified by NMR as the product of addition of MeOH to **2b**.<sup>1b</sup>
- (16) See, for example: (a) Fryzuk, M. D.; MacNeil, P. A.; Rettig, S. J. *Organometallics* **1985**, *4*, 1145 (Ir amido). Fryzuk, M. D.; Montgomery, C. D.; Rettig, S. J. *Organometallics* **1991**, *10*, 467 (Ru amido). Fryzuk, M. D.; Bhangu, K. *J. Am. Chem. Soc.* **1988**, *110*, 961 (Ir phosphido). Roddick, D. M.; Santarsiero, B. D.; Bercaw, J. E. *J. Am. Chem. Soc.* **1985**, *107*, 4670 (Hf phosphido). Dahlenburg, L.; Hock, N.; Berke, H. *Chem. Ber.* **1988**, *121*, 2083 (Rh phosphido).
- (17) Hartwig, J. F., *Organotransition Metal Chemistry: From Bonding to Catalysis*; University Science Books: Mill Valley, CA, 2010; p 602.
- (18) We searched carefully for minima and saddle points containing  $\eta^3$ -indenyl structures in this system and found none. The first transition state in Figure 2 shows considerable slip distortion ( $\Delta = 0.26 \text{ \AA}$ ) relative to the intermediate ( $\Delta = 0.16 \text{ \AA}$ ) and the second transition state ( $\Delta = 0.13 \text{ \AA}$ ), but it is still well outside the range for formal  $\eta^3$  coordination ( $\Delta = 0.69\text{--}0.80 \text{ \AA}$ ): Cadierno, V.; Diez, J.; Gamasa, M. P.; Gimeno, J.; Lastra, E. *Coord. Chem. Rev.* **1999**, *193*–5, 147.
- (19)  $^{31}\text{P}\{^1\text{H}\}$  shifts and  $^2J_{\text{PP}}$  values for **8c,d** are similar to those previously observed for **8a**.<sup>1a</sup>
- (20) Due to the complexity of the aromatic region of the  $^1\text{H}$  NMR spectra, we were unable to identify signals due to coordinated (**7c,d**) or free (**8c,d**) benzonitrile in these samples.
- (21) Morrow, K. M. E.; Pantazis, D. A.; McDonald, R.; Rosenberg, L. Manuscript in preparation.

(22) Programs for diffractometer operation, unit cell indexing, data collection, data reduction and absorption correction were those supplied by Bruker.

(23) Beurskens, P. T.; Beurskens, G.; de Gelder, R.; Smits, J. M. M.; Garcia-Granda, S.; Gould, R. O. *The DIRDIF-2008 Program System*; Crystallography Laboratory, Radboud University, Nijmegen, The Netherlands, 2008.

(24) Sheldrick, G. M. *Acta Crystallogr.* **2008**, *A64*, 112.

(25) (a) Perdew, J. P.; Burke, K.; Ernzerhof, M. *Phys. Rev. Lett.* **1996**, *77*, 3865. (b) Perdew, J. P.; Burke, K.; Ernzerhof, M. *Phys. Rev. Lett.* **1997**, *78*, 1396.

(26) (a) Douglas, M.; Kroll, N. M. *Ann. Phys.* **1974**, *82*, 89.

(b) Jansen, G.; Hess, B. A. *Phys. Rev. A* **1989**, *39*, 6016.

(27) Weigend, F.; Ahlrichs, R. *Phys. Chem. Chem. Phys.* **2005**, *7*, 3297.

(28) Pantazis, D. A.; Chen, X. Y.; Landis, C. R.; Neese, F. J. *Chem. Theory Comput.* **2008**, *4*, 908.

(29) Neese, F. *ORCA-an ab initio, Density Functional and Semi-empirical Program Package, 2.8.0*; Universität Bonn, Bonn, Germany, 2010.